

 Open access • Journal Article • DOI:10.1063/1.110016

Small-signal gain measurements in an electron beam pumped F2 laser

— [Source link](#) 

Hubertus M.J. Bastiaens, B.M.C. van Dam, P.J.M. Peters, W.J. Witteman

Published on: 26 Jul 1993 - Applied Physics Letters (American Institute of Physics)

Topics: Gas laser, Laser, Power density and Coaxial

Related papers:

- [An efficient, high-power F2 laser near 157 nm](#)
- [vuv emissions from mixtures of F2 and the noble gases—A molecular F2 laser at 1575 Å](#)
- [Efficiency characterization of vacuum ultraviolet molecular fluorine \(F/sub 2/\) laser \(157 nm\) excited by an intense electric discharge](#)
- [Discharge Pumped F_sub.2 Laser at 1580 Alpha](#)
- [Long pulse electron beam pumped molecular f2* laser](#)

Share this paper:    

View more about this paper here: <https://typeset.io/papers/small-signal-gain-measurements-in-an-electron-beam-pumped-f2-3dprlxkew>

Small-signal gain measurements in an electron beam pumped F_2 laser

H. M. J. Bastiaens, B. M. C. van Dam, P. J. M. Peters, and W. J. Witteman

University of Twente, Department of Applied Physics, P.O. Box 217, 7500 AE Enschede, The Netherlands

(Received 1 December 1992; accepted for publication 11 May 1993)

The net-small-signal gain of a molecular fluorine F_2^* laser pumped by a coaxial electron beam has been measured in gas mixtures of He/ F_2 and He/Ne/ F_2 . A peak net-small-signal gain of 0.63 cm^{-1} has been measured in a mixture of He/Ne/ F_2 at a pressure of 8 bar and a pumping power density of 13 MW/cm^3 .

There is considerable interest in the molecular F_2^* laser as it is a powerful laser source in the vacuum ultraviolet (VUV). The molecular F_2^* laser emits 157 nm radiation which, for instance, can be applied in high-resolution lithography, photochemical vapor deposition, photoablation, and efficient x-ray production. The molecular F_2^* laser was demonstrated first by Rice, Hays, and Woodworth by using long pulse electron beam excitation.¹ Shortly thereafter the same authors showed that efficient operation is also possible for a relatively short but intense pumping pulse.² Almost a decade later, Obara and co-workers published some papers on the theory of the electron beam pumped as well as on the discharge pumped F_2^* laser.^{3,4} Since then there is a renewed interest in the F_2^* gas discharge laser.^{5,6}

Important parameters like the gain and the saturation intensity of the F_2^* laser medium have not been fully evaluated. Up till now a few measurements have been reported.^{7,8} These data on gain and saturation intensity have been collected from experiments in gas discharge systems. In this letter the results of gain measurements in an electron beam pumped F_2^* laser for different gas mixtures will be described.

The small signal gain in the electron beam pumped section is measured in an oscillator/amplifier configuration where a discharge device provides the probe laser beam. The experimental setup is shown in Fig. 1.

The discharge device is a capacitively coupled F_2^* laser. In this device an ionizing front propagates inside along the discharge tube and excites the laser medium.⁹⁻¹¹ The device is powered by a Marx generator delivering a high voltage pulse of 150 kV, a rise time of 13 ns and a pulse width of about 30 ns. It has been successfully applied for the KrF laser with an output energy of 2 mJ, the ArF laser with an output energy of 0.5 mJ, and for the N_2 laser with an output energy of 200 μJ . With a He/ F_2 gas mixture this system yields an output energy of 80 μJ for the VUV molecular fluorine laser transition from a cavity with a MgF_2 output coupler and an Al end reflector. In Fig. 2(a) a typical probe laser signal is shown. The laser pulse width is 20 ns (FWHM). The laser wavelength is measured to be $157.6 \pm 0.5 \text{ nm}$. The small-signal gain is measured in an amplifier section which is pumped by a coaxial electron beam.¹² The laser gas is contained in a titanium tube with a diameter of 10 mm and a wall thickness of 25 μm . The excitation length is only 4 cm to avoid saturation of the medium by amplified spontaneous emission. The current pulse measured inside the Ti tube has a width of 25 ns

(FWHM) as shown in Fig. 3. The power deposition measured by a pressure jump technique is $1 \text{ MW/cm}^3/\text{bar}$ for He and $2.5 \text{ MW/cm}^3/\text{bar}$ for Ne. At both ends of the amplifier section MgF_2 windows are mounted under an angle with the optical axis in order to avoid optical feedback into the amplifier.

The probe laser beam diverges and within the physical dimensions of the experimental setup the diameter of the probe beam will be too large to travel freely through the amplifier. Therefore, the beam is converged with a MgF_2 lens. The minimal beam width and the highest intensity is reached in the middle of the amplifier section. The maximum input intensity calculated at 30 kW/cm^2 is far below the saturation intensity as measured by Skordoulis, Spyrou, and Cefalas.⁷ Therefore, in this configuration the small-signal gain will be measured.

The detectors 1 and 2 in Fig. 1 are silicon photodiodes (EG&G, FND 100 Q). The output of the probe laser is measured with a pyroelectric detector (Laser Precision RJP-735). To avoid absorption of the VUV radiation in the atmosphere the optical paths between the probe laser and the amplifier and to the detectors are flushed with very pure nitrogen (purity > 99 999%). In front of the detectors 1 and 2 scintillator material was placed to convert the VUV radiation into radiation with a wavelength that lies in the sensitivity range of the photodiodes.

In Fig. 2 a typical VUV laser signal from the probe laser is shown together with the amplified laser signal. The signal from the probe laser measured with detector 1 is corrected for a strong signal from the atomic fluorine laser coming from both the probe laser and the amplifier. The signal from the amplified probe laser measured with detector 2 is corrected for the molecular fluorine fluorescence signal coming from the amplifier section. The corrected amplified probe laser signal is shown in Fig. 2(b).

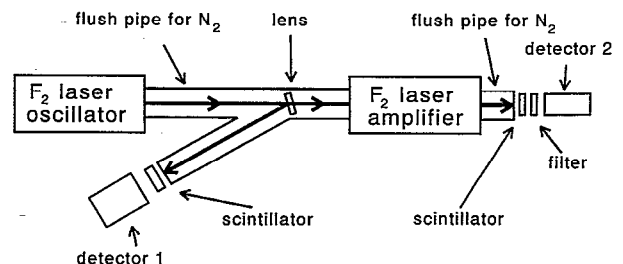


FIG. 1. Schematic representation of the experimental setup.

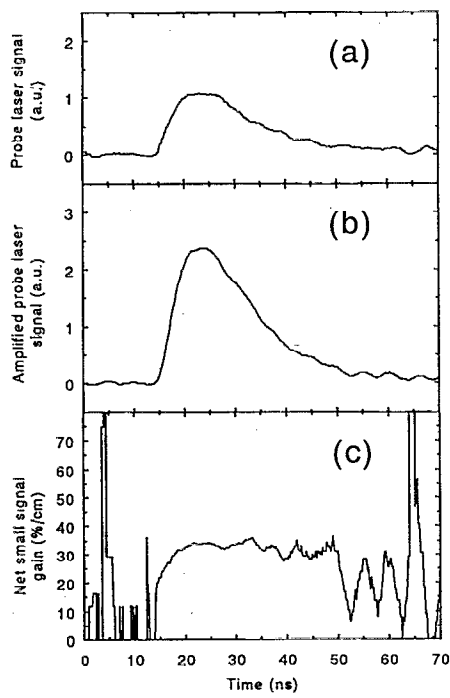


FIG. 2. (a) Temporal behavior of the probe laser signal injected into the amplifier. (b) Temporal behavior of the amplified probe laser signal. (c) Temporal behavior of the net-small-signal gain at 6 bar total pressure in a mixture of helium and 0.2% F_2 .

In the experiment the net-small-signal gain ($g_{0,net}$) is measured. It results from the small-signal gain minus the transient absorption created during excitation. The gain is calculated from $g_{0,net} = \ln(I_o/I_i)/l$ with I_o/I_i being the ratio of the output intensity (I_o) and the input intensity (I_i) and l being the active length of the amplifier. I_o is proportional to the signal of detector 2 and I_i is proportional to the signal of detector 1. With the amplifier section not activated, the absolute signal ratio of detectors 1 and 2 in a zero-gain situation is measured. In order to find the correct intensity ratio for the calculation of the gain the signal ratio has to be corrected with this absolute signal ratio.

The gain signal as shown in Fig. 2(c) is calculated

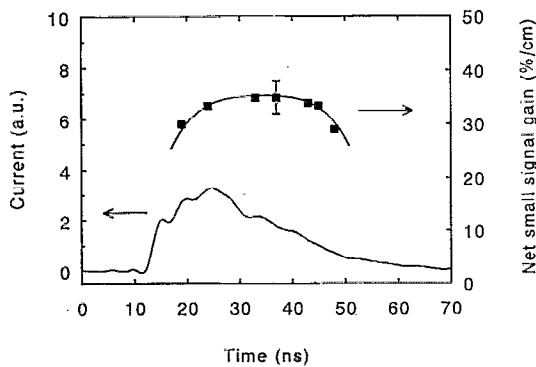


FIG. 3. Temporal behavior of the gain resulting from measurements in which the probe laser pulse is shifted in time through the gain pulse at 6 bar total pressure in a mixture of helium and 0.2% F_2 . Also shown is the temporal behavior of the current pulse which excites the laser medium in the amplifier.

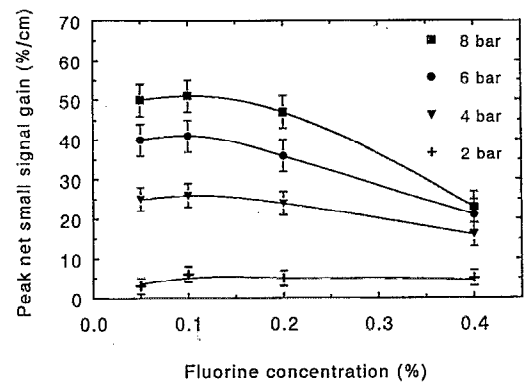


FIG. 4. Peak net-small-signal gain in a He/ F_2 gas mixture as a function of the fluorine concentration for various total pressures.

from the signals shown in Figs. 2(a) and 2(b) according to the formula given above. The large oscillations at the beginning and the end of the gain signal originate from the division of the noise on the probe laser signal by the noise of the amplified probe laser signal.

The temporal width of the net gain in the amplifier is measured in another way. The probe laser pulse is shifted in time through the gain pulse. The net gain is calculated at the peak of the probe laser pulse. The position of this peak is controlled by varying the trigger timing of the probe laser with respect to the trigger timing of the amplifier section. The results of these measurements are shown in Fig. 3 together with the current pulse measured inside the amplifier. The net gain shows a broad peak over almost 20 ns.

The gain data shown in Figs. 4 and 5 are the peak values of the gain signal with the gain signal being calculated from the probe laser signal and the amplified probe laser signal as is done for Fig. 2(c). By controlling the trigger timing of the probe laser, the probe laser pulse is injected at the center of the gain pulse. Each point in Figs. 4 and 5 is an average value over three shots with a fresh gas fill in the amplifier for every shot.

In Fig. 4 the peak net-small-signal gain in a He/ F_2 gas mixture is shown as a function of the fluorine fraction for various total gas pressures. The gain shows an optimum around 0.1% F_2 at the various pressures. As can be seen

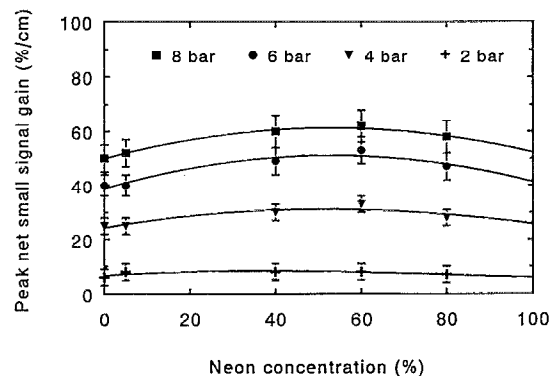


FIG. 5. Peak net-small-signal gain in a He/Ne/ F_2 gas mixture with 0.1% F_2 as a function of the neon concentration for various total pressures.

indirectly, the gain also increases almost linearly with increasing pressure.

In Fig. 5 the peak net-small-signal gain is shown as a function of the neon fraction of the He/Ne/F₂ gas mixture with 0.1% F₂ for various total gas pressures. From this figure it can be seen that the gain increases when neon is added to a helium based mixture. With the addition of more neon than the optimal fraction of 60% the gain decreases to roughly the same value as of the helium based mixture. The maximum peak net-small-signal gain found is to be 63%/cm for a mixture with 60% Ne at a total gas pressure of 8 bar.

If the pressure of the He/F₂ mixture in the amplifier is increased as also shown in Fig. 4 the energy deposited by the electron beam is increased. This results in a higher pumping rate for the upper laser level and most likely results in the higher gain as seen in this figure. The observation that there is an optimum in the F₂ concentration as shown in Fig. 3 is probably due to an increased absorption of F⁻ above this optimum value.

Replacing helium by neon in the gas mixture of the amplifier section offers the advantage of the higher power deposition by the electron beam in neon than in helium which might result in a higher pumping rate for the upper laser level and eventually in a higher gain. Experimentally we see that adding neon to a He/F₂ gas mixture up to a fraction of 60% neon indeed results in an increase of the gain.

Since the increase of the gain with higher neon concentration is not proportional to the increased power deposition and since this gain reaches a maximum at a concentration of about 60% neon we may conclude that neon has a strong quenching effect on the kinetic chain which leads to inversion in the F₂^{*} laser medium. However, for a

complete evaluation of the value of the addition of neon we also need to know the saturation intensity as a function of the neon concentration. This will be our next experimental goal.

We have shown that the net-small-signal gain in an electron beam pumped F₂^{*} amplifier can be measured with a probe laser in an oscillator/amplifier configuration. The gain measured in an electron beam pumped amplifier is found to be very high. For mixtures of He and 0.1% F₂ we measured a gain of roughly 50%/cm at 8 bar total gas pressure and a pumping power density of 8 MW/cm³. For mixtures of He/Ne/F₂ with 60% Ne and 0.1% F₂ we measured a gain of about 60%/cm at 8 bar total pressure and a pumping power density of 13 MW/cm³.

¹J. K. Rice, A. K. Hays, and J. R. Woodworth, *Appl. Phys. Lett.* **31**, 31 (1977).

²J. R. Woodworth and J. K. Rice, *J. Chem. Phys.* **69**, 2500 (1978).

³Y. P. Kim, M. Obara, and T. Suzuki, *J. Appl. Phys.* **59**, 1815 (1986).

⁴M. Ohwa and M. Obara, *Appl. Phys. Lett.* **51**, 958 (1987).

⁵K. Yamada, K. Miyazaki, T. Hasama, and T. Sato, *Appl. Phys. Lett.* **54**, 597 (1989).

⁶M. Kakehata, T. Uematsu, F. Kannari, and M. Obara, *IEEE J. Quantum Electron.* **QE-27**, 2456 (1991).

⁷C. Skordoulis, S. Spyrou, and A. C. Cefalas, *Appl. Phys. B* **51**, 141 (1990).

⁸M. Kakehata, C. H. Yang, Y. Ueno, F. Kannari, and M. Obara, in *Digest of CLEO'92* (Optical Society of America, Washington, DC, 1992), p. 110.

⁹T. Gerber, P. J. M. Peters, and H. M. J. Bastiaens, *Opt. Commun.* **53**, 401 (1985).

¹⁰E. I. Asinovskii, L. M. Vasilyak, and V. V. Markovets, *High Temp. (USA)* **21**, 293 (1983).

¹¹E. I. Asinovskii, L. M. Vasilyak, and V. V. Markovets, *High Temp. (USA)* **21**, 448 (1983).

¹²P. J. M. Peters, Y. F. Lan, M. Ohwa, and M. J. Kushner, *IEEE J. Quantum Electron.* **QE-26**, 1964 (1990).